Send Orders for Reprints to reprints@benthamscience.ae

The Open Remote Sensing Journal, **2015,** *6,* **1-10**

Estimation of Leaf Area Index of Hemiboreal Forests

Andres Kuusk[a,*], Mait Lang[a,b], Ave Kodar[a] and Allan Sims[b]

[a]*Tartu Observatory, 61602 Tõravere, Estonia*

[b]*Estonian University of Life Sciences, Kreutzwaldi 1, 51014 Tartu, Estonia*

Abstract: ACRM, a two-layer homogeneous canopy reflectance model is applied for the estimation of leaf area index (LAI) of forests using Proba/CHRIS spectral signatures and model inversion. A regularity parameter is used in the model in order to account for the grouping of foliage into tree crowns. Results of LAI estimation at the Järvselja forested test site, in Estonia, are compared with ground truth readings available at the test site, and with LAI estimates by MODIS and MERIS/CYCLOPES LAI products for the test site. MODIS LAI estimates are systematically higher than MERIS estimates. The estimated LAI values from ACRM inversion using CHRIS data have wider range than MODIS and MERIS estimates for the test site because of smaller pixel size. In general, LAI values from CHRIS data are between MODIS and MERIS LAI values, however, systematically lower than allometric LAI of forest stands using forest inventory data and regressions suggested for the boreal zone in literature.

Keywords: ACRM, LAI, Forest, Reflectance model inversion.

1. INTRODUCTION

Among many vegetation characteristics, leaf area index (LAI) is of prime importance. It controls light interception and relevant processes such as photosynthesis, energy balance, carbon fluxes, and water balance. Direct measurement of LAI by measuring the area of all leaves in a forest and/or landscape is unthinkable. Even optical ground measurements (LAI-2000, hemispherical photos) are too labor-intensive for the estimation of LAI for large areas as they can provide only point estimates of LAI. Optical methods provide biased estimates of LAI which can be corrected by regression formulae, however, this relationship is nonlinear and regression parameters depend on the stand structure [1]. Allometric regressions can be applied only for forests for which forest mensuration data are available and up to date. Even then, allometric regressions can not account for all site characteristics such as site fertility, stand density, previous management actions, etc. The convenient operational possibility to estimate LAI of forests and/or landscape is using aerial or satellite measurements. The observations with instruments like MODIS and MERIS are used for producing land cover products including LAI [2, 3]. The MERIS LAI product is carried out using CYCLOPES procedure [4]. Such procedures have been developed and validated for years, however, due to the complexity of the problem, recent comparisons of MODIS and CYCLOPES LAI products by Fang *et al.* [5] concluded that the uncertainties in LAI products are still around $\pm$ 1.0 LAI units.

*Address correspondence to this author at the Tartu Observatory, 61602 Tõravere, Estonia; Fax: +372-696-2555; E-mail: andres@to.ee

Alternative methods of LAI estimation using multiple sources, multiple view directions, airborne lidar data etc are under development [6-11]. The increasing number of satellite information and increasing spatial resolution of satellite sensors encourage to develop new computationally effective methods of LAI estimation.

In a paper by Kuusk [12] a homogeneous canopy reflectance (CR) model was used for the estimation of landscape LAI by inversion using Landsat TM spectral signatures in shortwave bands TM2--TM5 and TM7. A newer version of the same CR model [13] was used by Liu *et al.* [14] for the LAI estimation at six study sites using MODIS, CYCLOPES, and MISR reflectance data. The study sites included cropland, grassland, and a forest site of deciduous trees in Germany. This study was oriented towards the development of methods for building global LAI products.

The comparison of estimated LAI map with land use map in Kuusk [12] shows that the estimation of forest LAI by the inversion of a homogeneous CR model fails. The LAI of forests was obviously underestimated, especially that of conifer forests. In the Landsat scene forests are darker than grasslands and green field crops in all spectral bands. The comparison of CR simulations by a forest CR model and homogeneous model in Kuusk *et al.* [15] shows that the aggregation of foliage into tree crowns makes the scene darker. The grouping of foliage into tall tree crowns increases the amount of visible shadows in a scene. This is the reason of bias in LAI estimation in forests by the inversion of homogeneous CR models which do not account for this characteristic structure of a forest canopy.

1875-4139/15

Houborg *et al.* [16] suggested a simple, but very *ad hoc* scheme, how to use the two-layer homogeneous CR model ACRM by Kuusk [13] for the estimation of forest parameters by the inversion of the model. Instead of analyzing why the model fails over forests the measured forest spectral reflectance was corrected by an empirical factor derived using differences of the normalized difference vegetation index (NDVI) over crop fields and forests.

Several forest reflectance models have been developed which can be inverted using CR spectra [17]. Such models have a long list of input parameters. This makes the estimation of forest LAI by the inversion of such models problematic. Numerous free parameters create high degree of freedom in the model inversion. Typically, there is not sufficient information available for estimating simultaneously all these parameters by the inversion of a forest reflectance model, and various combinations of model input parameter values may provide equal fit of simulated and recorded spectral signatures. Inversion of such a model is a typical ill-posed problem, which can be solved only by fixing several model parameters to expert values [18]. Only a few parameters can be left free in inversions. Unfortunately, errors in fixed parameter values result in biased LAI estimates in the inversion of a forest reflectance model.

In the present work a new attempt is made to estimate forest LAI by the inversion of a few-parameter homogeneous CR model. In the two-layer homogeneous model ACRM the regularity of foliage pattern in forests caused by grouping foliage into tree crowns is accounted for by a clumping/regularity parameter. A procedure is defined for estimating the LAI of hemiboreal forests at a sub-satellite test site in Estonia by the inversion of the model using medium resolution CHRIS/Proba (17 m) and Hyperion (30 m) spectral signatures. Inversion results are compared to MODIS and MERIS land products, and to ground truth measurements at several test plots in the test site.

2. DATA

Forest data have been collected at the Järvselja Training and Experimental Forestry District (Estonia, 58.30 ° N, 27.26 °E). The Forestry District has served as a test site for the CHRIS/PROBA mission [19] and VALERI effort [20]. Järvselja forests, located on a flat landscape at 50 m above sea level, are representative of the hemi-boreal zone. Stands are pure or mixed and composed mainly of silver birch (*Betula pendula*), Scots pine (*Pinus sylvestris*), Norway spruce (*Picea abies*), common alder (*Alnus glutinosa*), aspen (*Populus tremula*), white alder (*Alnus incana*), small-leaved lime (*Tilia cordata*). Growth conditions range from poor where the site index H_{100} (stand height at the stand age of 100 years) is less than 10 m to very good where H_{100} can be over 35 m. A more detailed description of the test site is provided by Kuusk *et al.* [21]. Forest stands in Järvselja are inventoried every ten years. The stand maps and description data base are compiled. The GIS database from year 2011 forest inventory contains several forest parameters such as species composition, age, diameter at breast-height, tree height, site type, etc for each stand. A forest stand is defined as a geographically unified area which has a relatively uniform species composition and is managed as a single unit. Three mature stands at the test site have been studied in detail previously, and the database of the forest structure and optical properties that is intended for forest radiative transfer modeling experiments, referred to as the Järvselja data-base, is built by Kuusk *et al.* [22-24]. Allometric LAI of tree canopy was calculated using specific leaf weight (SLW) from literature [25] and leaf mass regressions by Repola [26, 27] which link the tree layer LAI to tree height H and diameter at breast-height DBH, $LAI = N \cdot m(DBH, H)/SLW$, where N is the number of trees per square meter and $m(DBH, H)$ is leaf mass per tree. Dependent on the dominant stand species, seven different regression formulae for foliage mass are in use [23].

There are several smaller test plots at Järvselja which are used in various forestry studies. Leaf area index measurements with LAI-2000 plant canopy analyzer, and estimates using hemispherical photos and CAN_EYE software [28] at 42 elementary sampling units of the VALERI project carried out in 2009 are involved in the present study.

A successful CHRIS Mode 3 [19] acquisition of the test site was on July 5, 2010. CHRIS acquisition was supported by simultaneous spectroscopic measurements of atmosphere transparency, incident spectral radiation, and airborne measurements of top-of-canopy forest reflectance spectra. Two-stage atmospheric correction of CHRIS images for the conversion of satellite signals to the top-of-canopy reflectance factor was carried out as described in Kuusk et al. [29]. In the first stage the look-up-table (LUT) of satellite signal in CHRIS spectral bands was calculated using the atmospheric radiative transfer model 6S by Vermote et al. [30] and values of optical properties of the atmosphere from the spectral irradiance and sun-photometer measurements during acquisition. In the second stage the adjacency correction was performed by the spacial filtering of the 2D Fourier spectra of the spectral images of the test site.

Significant part of the CHRIS scene of July 5, 2010 is also covered by the Hyperion scene of August 18, 2005. Hyperion is a hyperspectral imager on board the earth observing satellite EO-1 [31]. 21 spectral bands suggested by Huang *et al.* [32] were used in this research.

MODIS Collection 5 LAI data [33] for the CHRIS acquisition date are available on-line [2]. MODIS LAI maps have 1 km × 1 km pixels.

MERIS LAI product is using the CYCLOPES algorithms [4]. LAI data for the test site is provided by the Geoland2 project, a Collaborative Project (2008-2012) funded by the European Union under the 7th Framework Programme [3]. The LAI product is available since 2011, data for July and August 2011 were used in this study. MERIS LAI maps have 300 m × 300 m pixels.

2.1. Forestry Data and Image Classification

The forestry data base was used for distinguishing between spruce, pine, and broadleaf stands, and grass. The stands younger than 5 years and open areas were considered grasslands. A stand was considered a spruce stand if the main species was spruce and there was less than 50% of broadleaf trees in the stand. Similar conditions were applied for pine stands. The rest of forests were considered broadleaf stands. These data are available only for stands registered in the forestry data base. Such stands cover 27% of the CHRIS scene CD78 of July 5, 2010 -- close to nadir scene. In order to distinguish between forest types and non-forest area in the whole scene, the scene was classified into 96 classes using 16 CHRIS spectral images. The non-supervised classification in the GRASS GIS [34] was used. Spectral bands 1 (blue) and 18 (992-1036 nm) which have the highest noise level were not used. Probabilities to fall into any class of spruce, pine or broadleaf stand were analyzed using the forestry data base.

3. INVERSION OF THE CANOPY REFLECTANCE MODEL

3.1. Clumping and Regularity of Foliage

The homogeneous CR model ACRM has no detailed description of the canopy structure. The only structure parameters are LAI, leaf angle distribution (LAD) described by the two-parameter elliptical distribution [35], the Ross-Nilson geometry function $G(\theta)$ -- the projection of unit leaf area in the direction θ, and the foliage clumping parameter γ. Single scattering canopy reflectance is controlled along with foliage and soil optical properties by the bidirectional gap fraction $a_{sv}(\theta_s, \theta_v)$ in Sun and view directions,

$$a_{sv}(\theta_s, \theta_v) = a(\theta_s)a(\theta_v)C_{HS}(\theta_s, \theta_v). \quad (1)$$

Here $a(\theta)$ is the gap fraction at zenith angle θ, and $C_{HS}(\theta_s, \theta_v)$ is the hot spot factor which accounts for the statistical dependence of gap probabilities in Sun and view directions [36].

The clumping of foliage changes the gap probability (and bidirectional gap probability) in a canopy. Foliage clumping modifies the Ross-Nilson geometry function $G(\theta)$ which controls, along with LAI, the gap fraction in a canopy [37]. The mutual obscuring of phytoelements in a clumped canopy decreases the G-function to an effective G-function, $G(\theta) \to G_{eff}(\theta) = \gamma G(\theta)$, where $\gamma < 1$, θ is the view zenith angle. The effective G-function and increase of canopy transparency due the clumping of foliage was introduced to the initial homogeneous CR model by Kuusk [35] in the Markov chain version of the model. The gap fraction is calculated as $a(\theta_j) = \exp(-LG_{eff}(\theta_j)/\mu_j), j = s, v, \mu = cos(\theta)$, θ_s and θ_v are Sun and view zenith angles, respectively, L is leaf area index, and the hot-spot factor $C_{HS}(\theta_s, \theta_v)$ is defined as [36]:

$$C_{HS}(\theta_s, \theta_v) = \exp\left(\int_0^z \sqrt{\frac{G_{eff}(\theta_s)G_{eff}(\theta_v)}{\mu_s\mu_v}}\, u_L(z')Y_{\xi_s,\xi_v}(l(z'))dz'\right). \quad (2)$$

Here $u_L(z')$ is the leaf area density and $Y_{\xi_s,\xi_v}(l(z'))$ is the cross correlation function of the indicator functions ξ_j, $j = s, v$, which describe the presence of leaves at the height z' in two points of distance $l(z') = (z - z')\sqrt{1/\mu_s^2 + 1/\mu_v^2 - 2\cos(\alpha)/(\mu_s\mu_v)}$ from each other, α is the angle between Sun and view lines of sight.

In a layered homogeneous canopy clumping of foliage ($\gamma < 1$) increases bidirectional gap probability $a_{sv}(\theta_s, \theta_v)$, and consequently canopy reflectance [35].

As has been shown in Kuusk [36], the cross correlation function $Y_{\xi_s,\xi_v}(l(z'))$ in Eq. (2) can be approximated by the autocorrelation function $Y_\xi(l(z'))$ of the indicator function $\xi = \xi(\theta = 0)$. Replacing in Eq. (1) expressions for gap fraction and hot spot factor the Eq. (1) gets the form

$$a_{sv}(\theta_s, \theta_v) = \exp(-LG_{eff}(\theta_s)/\mu_s - LG_{eff}(\theta_v)/\mu_v + J(\theta_s, \theta_v)), \quad (3)$$

where $J(\theta_s, \theta_v)$ is the integral in the exponent of Eq. (2). The last component in the exponent in Eq. (3) corresponds to the correction factor C_{HS} in Eq. (1).

In homogeneous vegetation canopies of finite leaf size, finite geometrical thickness of canopy, and of random foliage distribution the correlation $Y_\xi(l(z'))$ decreases monotonously from 1 to 0 as a function of distance. It can be approximated by an exponential function, correlation radius of which is determined by mean leaf size. In the hot spot $\theta_s = \theta_v, \alpha = 0$, and $J(\theta_s, \theta_s) = LG_{eff}(\theta_s)/\mu_s$. If the Sun and view direction are far from each other and foliage spacial pattern is random, then $J(\theta_s, \theta_v) \to 0$. The correction factor C_{HS} is not less than one.

An attempt to estimate correlation function $Y_\xi(l(z'))$ in the pine forest of Järvselja data-base was done using airborne lidar data [23]. Each green line in Fig. (**1**) denotes a random transect, and the solid blue line is the mean value of the autocorrelation function $Y_\xi(l(z'))$. The high frequency oscillation of the mean function (period about 0.9 m) is caused by the emitted pulse pattern in lidar data. Weak local minima at about 4 m and 12 m, and local maxima at about 7 m and 16 m are caused by the finite diameter of tree crowns and tree pattern in the stand.

If the main part of foliage is at the levels where the distance between Sun and view lines of sight $l(z')$ falls in the range where the correlation function $Y_\xi(l(z'))$ is negative then the integral $J(\theta_s, \theta_s)$ is negative. That means, the bidirectional gap probability $a_{sv}(\theta_s, \theta_v)$ is in such canopy less than in a random canopy - we see more shadows and the canopy looks darker than the random canopy of the same

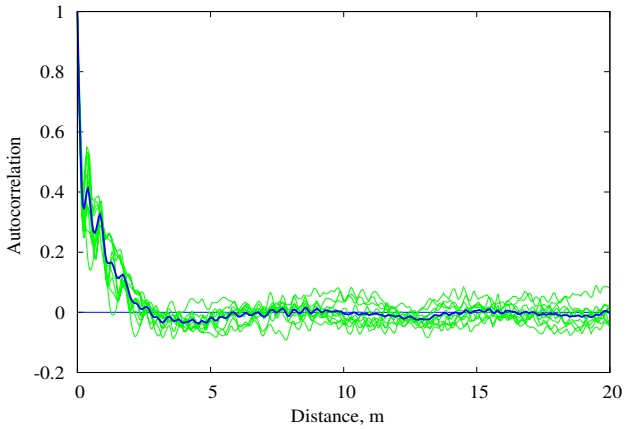

Fig. (1). Autocorrelation function of the airborne lidar signal in the Järvselja pine stand discriminated to an indicator function at the level $z = 5$ m. The solid blue line depicts the average value.

LAI and same optical properties of foliage. Obviously in forests the decrease of bidirectional gap probability caused by grouping of foliage into tree crowns and the tree pattern dominates over the increase of bidirectional gap probability due to the leaf-scale clumping and mutual shading of foliage in tree crowns. That can be accounted for by joining the clumping correction and grouping of foliage into tree crowns into the single clustering parameter γ. Using the analogy of the Markov models of canopy transparency introduced by Nilson [38], the clustering parameter γ is equal to 1 in random canopies, $\gamma < 1$ in clumped canopies, but in forests where foliage is grouped into tall tree crowns of significant vertical extent $\gamma > 1$,

$$a_{sv}(\theta_s, \theta_v) = \exp(-L(\gamma G(\theta_s)/\mu_s + G(\theta_v)/\mu_v)). \quad (4)$$

Looking vertically as the nadir-looking satellite images we do not see the sides of tree crowns, therefore $\gamma = 1$ is used for the view direction in Eq. (4).

3.2. Inversion of the Model

The two-layer homogeneous canopy reflectance model ACRM [13] is used for forests so that the upper layer represents the layer of tree crowns, and the lower layer the understorey vegetation. The value of the clustering parameter γ in the tree layer was estimated for a birch, pine, and spruce stand using data from the Järvselja data-base and CHRIS spectral signatures of July 5, 2010. There are four different LAI estimates in the Järvselja data-base - the allometric LAI, the effective LAI measured with LAI-2000, and two corrected LAI values using different algorithms to correct effective LAI [23]. Clustering parameter values were estimated by the inversion of the ACRM model so that leaf and ground vegetation parameters were fixed to the measured values and LAI values were fixed to these four estimated values. The respective clustering parameter estimates are γ_{all}, γ_{eff}, γ_1, and γ_2 in Table **1**.

We see that having fixed leaf optics and ground vegetation parameters, different LAI values return different estimate of the clustering parameter, and *vice versa*. The clustering parameter has its lowest value in the dense spruce forest, the intermediate value in the broadleaf forest, and the highest value in the pine forest where we have well separated tree crowns high above ground surface.

In the estimation of LAI by the inversion of ACRM in the whole scene 16 CHRIS bands and 21 Hyperion bands were used. Leaf area index was estimated separately for pine, spruce, and broadleaf stands, and grasslands. Effective leaf and needle optics parameters and understorey optics parameters were fixed dependent on forest type. Despite the thorough analysis of the angular dependence of gap fraction in mature forest stands by Kuusk *et al.* [39] suggest to use erectophile leaf angle distribution for the crown layer of mature forests, the LAD was fixed to spherical for all stands. In a forested landscape there are stands of various age, stand density, site fertility, species composition etc, therefore, there is no justification to fix the clustering parameter for a forest type (species) in the inversion. Also, the amount of understorey vegetation varies depending on the soil fertility and canopy cover of the tree layer. In the ACRM inversion three input parameters were left free -- LAI of the tree layer, the clustering parameter γ in the overstorey layer, and the LAI of ground vegetation. The clustering parameter γ was allowed to vary in the range 1.0-1.3 in spruce stands and in the range 1.0-1.4 in pine and broadleaf stands.

For non-forested areas the spherical leaf angle distribution was used, the clustering parameter was fixed to 1 and optical parameters of typical green leaves were used. The free parameters in the inversion were LAI and soil reflectance.

The allowed range for γ values was less than we see in Table **1**. The background of this restriction is the use of universal effective leaf optics parameters in all inversions of the given forest type. Forests of different age, density, and site fertility have different bark and stem area ratio to the green leaf area which modifies effective leaf reflectance and transmittance. We have no information to account for such differences. In the inversion the mismatch of effective

Table 1. Clustering parameter for different forest types.

Stand	LAI_{all}	γ_{all}	LAI_{eff}	γ_{eff}	LAI_1	γ_1	LAI_2	γ_2
Birch	3.93	1.55	2.94	1.45	3.14	1.46	2.89	1.45
Pine	1.86	1.87	1.75	1.89	2.55	1.78	2.21	1.81
Spruce	4.36	1.16	3.76	1.22	5.03	1.15	4.32	1.16

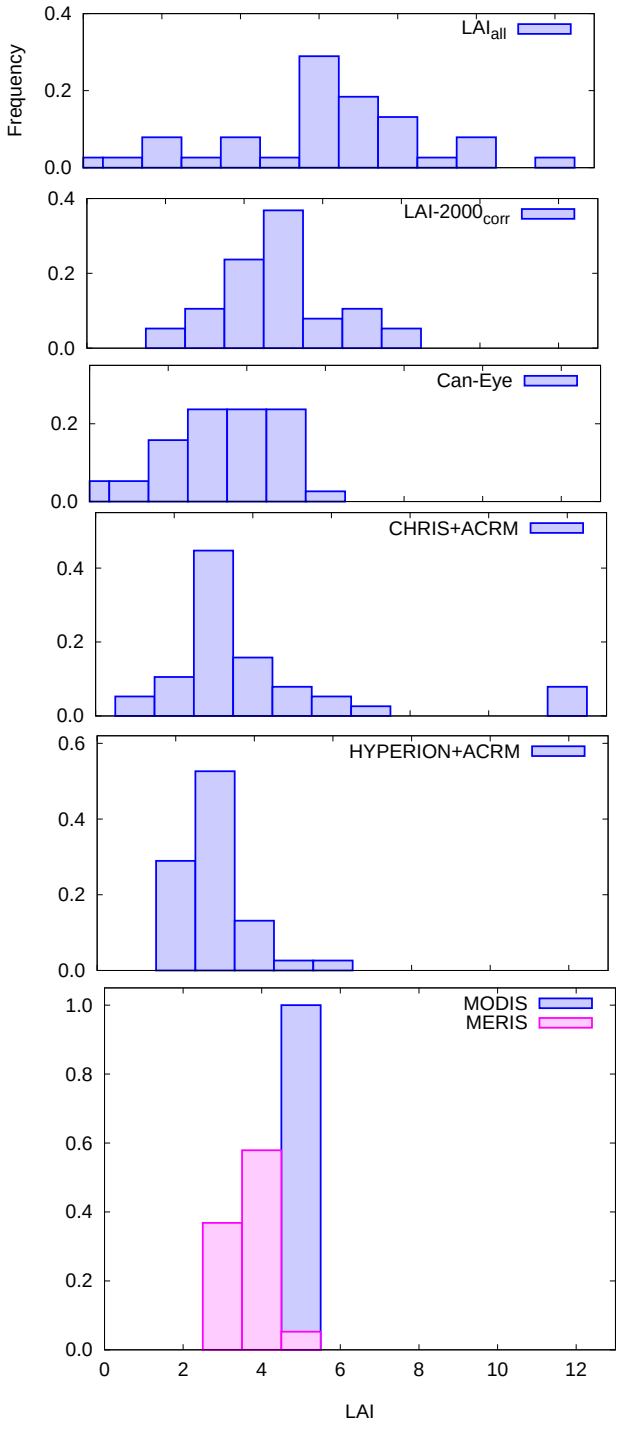

Fig. (2). Histograms of estimated LAI in VALERI elementary sampling units: LAI $_{all}$ - allometric LAI, LAI-2000 $_{corr}$ - effective LAI corrected by Nilson and Kuusk [40] algorithm, Can-Eye - LAI from hemispherical images, CHRIS+ACRM - inversion of CHRIS data of 05.07.2010, HYPERION+ACRM - inversion of Hyperion data of 18.08.2005, MODIS - MODIS LAI product of 1.-8.07.2010, MERIS - mean value of MERIS LAI products 1.07-31.08.2011.

optical parameters could be compensated by nonrealistic clustering parameter values if there is no restrictions to the range of γ values.

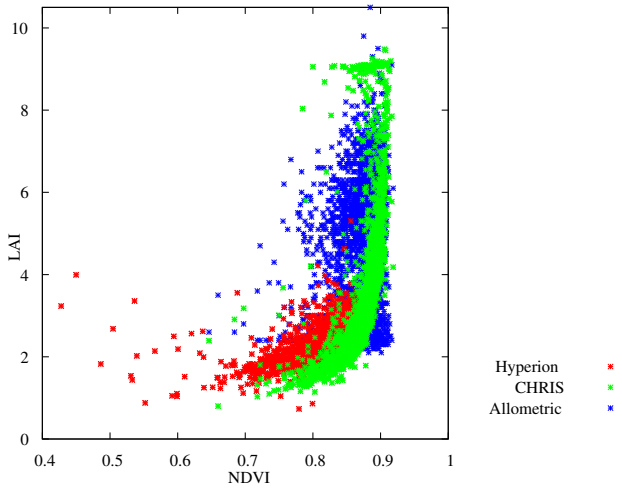

Fig. (3). Leaf area index of broadleaf stands estimated by ACRM inversion using CHRIS and Hyperion data, and allometric relations by Repola [26].

4. RESULTS

4.1. Elementary Sampling Units

The 42 elementary sampling units of the VALERI project are within the range both the CHRIS scene CD78 and Hyperion scene of August 18, 2005. Thus, the inversion of the CR model was run both using CHRIS data of July 5, 2010 and Hyperion data. LAI estimated by CR model inversion is compared to MODIS and MERIS LAI values, and LAI estimates based on LAI-2000 measurements and allometric regressions in Fig. (**2**). LAI estimated from CHRIS images is slightly higher than that from Hyperion images, and the variation of LAI values is higher. The 1 km pixels of MODIS LAI have the range 3.5-5.0. LAI values in MERIS LAI maps of 300 m resolution are systematically lower and have a wider range. Terrestrial LAI estimates from optical measurements have the range of values which is rather close to CHRIS-ACRM values, however, the stand-by-stand correlation is low. Allometric LAI values are higher than any of the optical LAI estimates.

4.2. Forest Stands

4.2.1. Broadleaf Stands

Leaf area index of 2245 broadleaf stands was estimated by the inversion of ACRM using CHRIS data and of 1299 stands using Hyperion data. Estimated stand total LAI (overstorey and understorey LAI) is plotted in Fig. (**3**) against NDVI together with allometric LAI using relations $LAI = LAI(D, H)$ by Repola [26] where D and H are breast-height diameter and tree height, respectively. In the allometric LAI the understorey LAI is accounted for as well. Using CHRIS data the NDVI was calculated using bands 14 (NIR, 777 nm) and 8 (red, 672 nm). Bands 43 (NIR, 783 nm) and 34 (red, 691 nm) of Hyperion were used for the NDVI of Hyperion data. LAI from CHRIS data reveals the typical

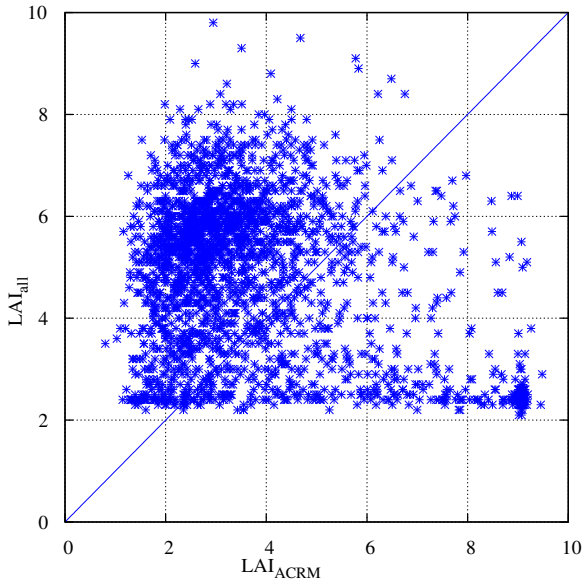

Fig. (4). Leaf area index of broadleaf stands estimated by ACRM inversion using CHRIS data, and allometric relations by Repola [26].

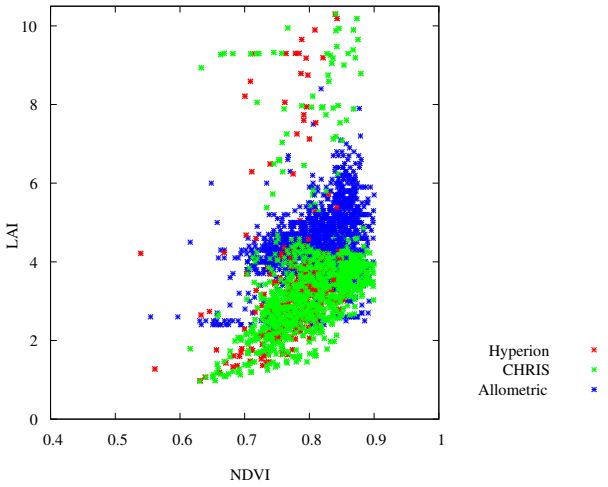

Fig. (5). Leaf area index of needle-leaf stands estimated by ACRM inversion using CHRIS and Hyperion data, and allometric relations by Repola [27].

nonlinear relationship to NDVI. A group of high LAI values at NDVI values less than 0.85 (about 4% of inversions) are the failed inversions of ACRM using CHRIS data. Involvement of shortwave NIR bands of Hyperion (bands 95 - 216) in the CR model inversion makes the results of inversion more stable and there are only few failed inversions. At the same time, the average value and the range of estimated LAI is smaller than using CHRIS data, and the relation between NDVI and estimated LAI is weaker. Allometric relations by Repola [26] return low LAI values also in case of high NDVI values and rather high LAI values in case of NDVI < 0.85 what is difficult to explain.

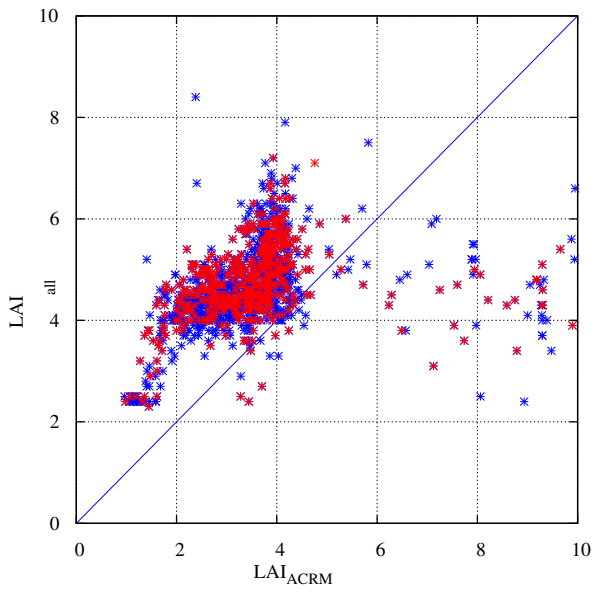

Fig. (6). Leaf area index of needle-leaf stands estimated by ACRM inversion using CHRIS (blue dots) and Hyperion (red dots) data, and allometric relations by Repola [27].

The estimated LAI from CR inversion using CHRIS data and from allometric relations by Repola [26] in Fig. (**4**) have similar range, however there is almost no correlation between these two LAI estimates, $r^2 = 0.08$.

4.2.2. Needle-leaf Stands

Leaf area index of 490 spruce stands and 636 pine stands estimated using CHRIS data, and of 238 spruce stands and 253 pine stands using Hyperion data together with allometric LAI is plotted against NDVI in Fig. (**5**). While CHRIS and Hyperion results are in the same range, the allometric LAI values are systematically higher, see also Fig. (**6**). The LAI-NDVI relation is not so pronounced as in case of broadleaf stands.

4.3. CHRIS Scene

For the estimation of LAI in the whole CHRIS scene the scene was classified into 96 classes and the ACRM was inverted four times separately on every class using effective optical parameters of pine, spruce or broadleaf stands, or of grass. The estimated LAI was calculated as the weighed mean of these four LAI estimates having the probabilities of every four land cover type in a class as the weight, Fig. (**7**). None of the stand in the forestry database falls into classes 77 and 96, grassland type was assigned to these signature classes. The LAI map generated this way is in Fig. (**8**). In Fig. (**9**) the histogram of estimated LAI values in the CHRIS scene is compared to the LAI histograms from MODIS and MERIS LAI products of the same area.

The distribution of LAI values over the same area using different estimation methods is very different. The mean LAI

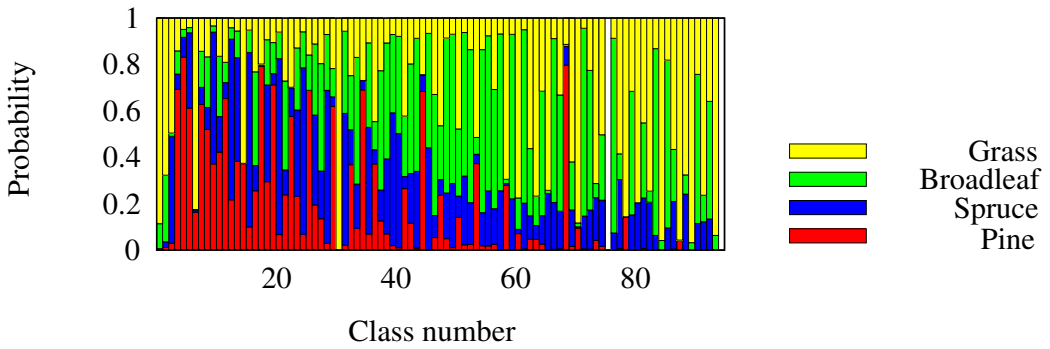

Fig. (7). Distribution of land-cover types between spectral signature classes.

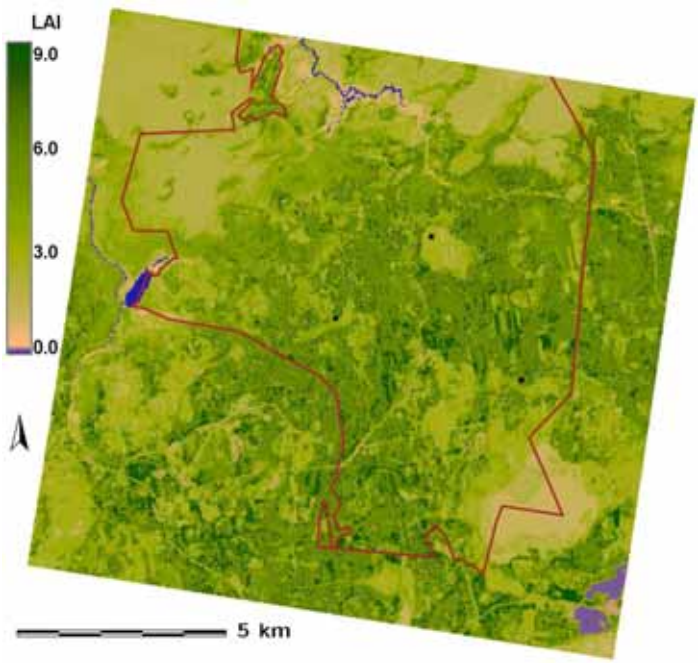

Fig. (8). LAI map of the CHRIS scene CD78, 5 July 2010, estimated by the inversion of ACRM canopy reflectance model using CHRIS spectral signatures. Brown line is the boundary of the Järvselja Training and Experimental Forestry District. The black dots mark the stands of the Järvselja data-base [22].

Table 2. Statistical parameters of LAI estimates in the CHRIS scene.

LAI Product	Pixel Size	Mean	STD
ACRM/CHRIS	17 m	4.19	1.91
MERIS	300 m	3.30	0.80
MODIS	1 km	4.75	1.24

and standard deviation (STD) are listed in Table **2**. While differences in the dispersion of estimated LAI values may be caused by differences in pixel size -- 1 km of MODIS LAI product, 300 m of MERIS LAI product, and 17 m in the CHRIS image, such differences in pixel size do not explain differences of the mean LAI over the 17 km × 17 km scene. The MERIS LAI values are systematically less than MODIS values, and the distribution is not so wide. The Kolmogorov--Smirnov and chi-square tests [41] in pair-vise comparisons of these distributions show that these distributions are not consistent, tests return strictly $p = 0$.

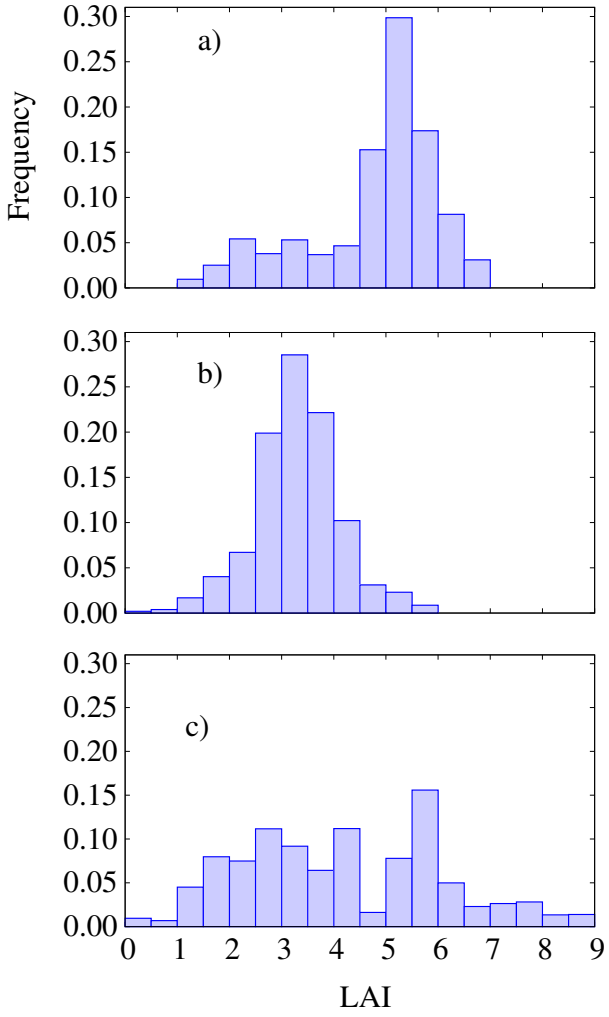

Fig. (9). LAI histograms of the CHRIS scene; a) MODIS LAI product, LAI $_{mean}$ = 4.8; b) MERIS LAI product, LAI $_{mean}$ = 3.3; c) ACRM inversion using CHRIS data, LAI $_{mean}$ = 4.2.

5. DISCUSSION AND CONCLUSION

The homogeneous two-layer canopy reflectance model ACRM [13] was applied for the estimation of leaf area index of the hemiboreal forested landscape using Proba/CHRIS Mode 3 spectral images of the test site. Land cover types were grouped into four classes - spruce, pine and broadleaf forests, and grassland. Cover type specific effective optical parameters were used for the overstorey layer of forests. The understorey vegetation was considered typical green vegetation of the region, and only the LAI of understorey was allowed to vary in the inversion. In the overstorey layer effective optical parameters of foliage consider the share of branches. The grouping of foliage into tree crowns of significant vertical extent is a kind of regularity in the three-dimensional foliage pattern. This regularity was accounted for in the effective geometry function $G_{eff}(\theta)$ by the regularity parameter $\gamma > 1$ which along with leaf area index controls the bidirectional gap fraction of the overstorey canopy. The estimated total leaf area index of understorey and overstorey of stands is compared to the ground truth estimates at elementary sample units of the VALERI project, to the allometric LAI estimates of stands described in the forestry data base, to the MODIS and MERIS LAI estimates, and to the LAI estimates by ACRM inversion using Hyperion data where Hyperion and CHRIS images overlap (53% of the CHRIS scene). Hyperion data were acquired five years earlier which may explain some differences in LAI values, however there has been no drastic change in land use in the region in last five or ten years which could cause significant changes in land cover in the whole scene.

The data sources in use have very different spatial resolution. Ground truth measurements are virtually point data. Pixel sizes of satellite images vary from 17 m (0.03 ha -- CHRIS) to 30 m (0.09 ha -- Hyperion), 300 m (9 ha -- MERIS LAI product), and 1 km (100 ha -- MODIS LAI product). The average size of stands in the forestry data base is 2.1 ha, however the standard deviation of the stand size distribution is 5.0 ha, thus the whole scale of stand sizes from 0.03 ha to more than 200 ha is rather equally represented. Therefore, large pixels of satellite products are mixed pixels in the sense of cover type, but not necessarily of varying LAI inside a pixel. In the analysis of CHRIS images the mixed pixels can be avoided using the buffered stand polygons. In Hyperion images the small stands have numerous mixed pixels. In MERIS and MODIS LAI maps every pixel is an average over several stands, as a rule.

Both the MODIS and MERIS LAI products base on solid algorithms, however these products over the same scene of forested landscape are different. While the validation of MODIS and MERIS (CYCLOPES) LAI products using global field measurement data by Fang *et al.* [5] revealed LAI differences around $\pm$ 1.0 LAI units, here we see even higher discrepancies. There is no criteria which one we should consider more reliable, even the *in situ* optical and allometric LAI estimates in the elementary sampling units of the VALERI project are totally different. The MODIS LAI values are systematically higher than MERIS and CHRIS estimates while the overlapping of MERIS and CHRIS LAI histograms is better. At the same time the allometric LAI estimates exceed the CHRIS estimate and overlap MODIS data in average. Surprisingly, the stand by stand correlation of allometric and CHRIS LAI estimates is very low while in the average these two LAI estimates are not so different: 4.9 and 3.7 in broadleaf stands, 4.3 and 3.0 in pine stands, and 4.9 and 5.5 in spruce stands, respectively. The almost missing dependence of NDVI on the allometric LAI in broadleaf stands (Fig. **3**) arouses suspicions in the reliability of the allometric method.

Rather similar attempt to estimate LAI of forest stands is in the paper by Schlerf and Atzberger [8] where spectro-directional CHRIS Mode 1 observations (62 spectral bands, 34 m pixels in nadir), the Invertible Forest Reflectance Model INFORM, and look-up-table method were used. The estimated LAI values of 15 Norway spruce stands and 13 stands of European beech at the Idarwald, Germany, exceed our CHRIS estimates in the average. The main differences in the procedures are as follows. The test site in the CHRIS scene at Järvselja includes the whole possible range of stand

age, growth conditions, and species composition. The elementary sampling units of the VALERI project are also selected to represent the whole variety of stands of the test site. In the experiment by Schlerf and Atzberger [8] the stands large enough and with relatively homogeneous canopy structure were selected. The involvement of off-nadir observations increased the stability of LAI estimation. This is the case only if the CR model reproduces well directional variations of forest reflectance. This may be problematic even in heterogeneous vegetation radiative transfer models [39] -- in order to adequately reproduce the asymmetry of radiation scattering in conifer canopies the Ross-Nilson phase function of foliage had to be replaced by the Henyey-Greenstein phase function.

The comparison of the LAI estimation using the simple two-layer homogeneous CR model ACRM to other indirect methods confirms that the inversion of the ACRM provides comparable LAI estimates of hemiboreal forested landscape if the regularity of foliage 3D pattern in forests is accounted for. The processing time of the 16 band 744×744 pixel CHRIS scene on a 3 GHz Linux PC was: 25.2 s image classification in GRASS-7.0, 18.2 s the inversion of ACRM on 96 spectral signatures. Thus, the method is operational on every PC and can be used for the monitoring of LAI seasonal or year-to-year changes on large forested areas using satellite images of moderate or even high spatial resolution.

CONFLICT OF INTEREST

The authors confirm that this article content has no conflict of interest.

ACKNOWLEDGMENTS

The CHRIS image data have been provided by the European Space Agency, using the ESA PROBA platform and the Surrey Satellite Technology Ltd instrument.

The MODIS LAI data were obtained through the online Data Pool at the NASA Land Processes Distributed Active Archive Center (LP DAAC), USGS/Earth Resources Observation and Science (EROS) Center, Sioux Falls, South Dakota (http://lpdaac.usgs.gov/get_data).

The MERIS LAI products are provided by Spot Image and Geoland2 project.

The forestry mensuration data are provided by Järvselja Training and Experimental Forest Center.

The study has been supported by Estonian Science Foundation, by Targeted financing by the Ministry of Education and Research, Project SF0180009Bs11, and by the EU Regional Development Foundation, Environmental Conservation and Environmental Technology R&D Programme project BioAtmos (3.2.0802.11-0043).

REFERENCES

[1] Mason EG, Diepstraten M, Pinjuv GL, Lasserre JP. Comparison of direct and indirect leaf area index measurements of Pinus radiata D. Don. Agric For Meteorol 2012; 166-167: 113-19.

[2] MODIS. Leaf area index - fraction of photosynthetically active radiation 8-Day L4 global 1km; 2010. Available from: https://lpdaac.usgs.gov/products/modis_products_table/leaf_area_index_fraction_of_photosynthetically_active_radiation/8_day_l4_global_1km/mod15a2.

[3] Geoland2. Biophysical Parameters Products; 2010. Available from: http://www.geoland2.eu/index.jsp

[4] Baret F, Weiss M. BioPar Methods Compendium. LAI, FAPAR, FCOVER, NDVI. Geoland2 Consortium; 2010. Available on-line http://web.vgt.vito.be/documents/BioPar/g2-BP-RP-BP038-ATBD_VegetationVariables_INRA-I1.5.pdf

[5] Fang H, Wei S, Liang S. Validation of MODIS and CYCLOPES LAI products using global field measurement data. Remote Sens Environ 2012; 119: 43-54.

[6] Yang G, Zhao C, Liu Q, Huang W, Wang J. Inversion of a radiative transfer model for estimating forest LAI from multisource and multiangular optical remote sensing data. IEEE Trans Geosci Remote Sens 2011; 49(3): 988-1000.

[7] Atzberger C, Richter K. Spatially constrained inversion of radiative transfer models for improved LAI mapping from future Sentinel-2 imagery. Remote Sens Environ 2012; 120: 208-18.

[8] Schlerf M, Atzberger C. Vegetation structure retrieval in beech and spruce forests using spectrodirectional satellite data. IEEE J Sel Top Appl Earth Observ Remote Sens 2012; 5(1): 8-17.

[9] Qi YJ, Li FR, Liu ZL, Jin GZ. Impact of understorey on overstorey leaf area index estimation from optical remote sensing in five forest types in northeastern China. Agric For Meteorol 2014; 198: 72-80.

[10] Ma H, Song JL, Wang JD, Xiao ZQ, Fu Z. Improvement of spatially continuous forest LAI retrieval by integration of discrete airborne LiDAR and remote sensing multi-angle optical data. Agric For Meteorol 2014; 189: 60-70.

[11] Moeser D, Roubinek J, Schleppi P, Morsdorf F, Jonas T. Canopy closure, LAI and radiation transfer from airborne LiDAR synthetic images. Agric For Meteorol 2014; 197: 158-68.

[12] Kuusk A. Monitoring of vegetation parameters on large areas by the inversion of a canopy reflectance model. Int J Remote Sens 1998; 19(15): 2893-905.

[13] Kuusk A. A two-layer canopy reflectance model. JQSRT 2001; 71(1): 1-9.

[14] Liu Q, Liang S, Xiao Z, Fang H. Retrieval of leaf area index using temporal, spectral, and angular information from multiple satellite data. Remote Sens Environ 2014; 145: 25-37.

[15] Kuusk A, Nilson T, Kuusk J, Lang M. Reflectance spectra of RAMI forest stands in Estonia: simulations and measurements. Remote Sens Environ 2010; 114(12): 2962-9.

[16] Houborg R, Soegaard H, Boegh E. Combining vegetation index and model inversion methods for the extraction of key vegetation biophysical parameters using Terra and Aqua MODIS reflectance data. Remote Sens Environ 2007; 106(1): 39-58.

[17] Widlowski JL, Taberner M, Pinty B, *et al*. Third radiation transfer model intercomparison (RAMI) exercise: documenting progress in canopy reflectance models. J Geophys Res Atmos 2007; 112(D9): D09111.

[18] Combal B, Baret F, Weiss M, *et al*. Retrieval of canopy biophysical variables from bidirectional reflectance using prior information to solve the ill-posed inverse problem. Remote Sens Environ 2002; 84(1): 1-15.

[19] Barnsley MJ, Settle JJ, Cutter MA, Lobb DR, Teston F. The PROBA/CHRIS mission: a low-cost smallsat for hyperspectral multiangle observations of the Earth surface and atmosphere. IEEE Trans Geosci Remote Sens 2004; 42(7): 1512-20.

[20] VALERI. VALERI; 2005. Available from: http://www.avignon.inra.fr/valeri/

[21] Kuusk A, Lang M, Nilson T. Forest test site at Järvselja, Estonia. Proceedings of the 3rd Workshop CHRIS/Proba, 21-23 March 2005; Frascati, Italy; European Space Agency (ESA) ESA-SP-593.

[22] Kuusk A, Kuusk J, Lang M. A dataset for the validation of reflectance models. Remote Sens Environ 2009; 113(5): 889-92.

[23] Kuusk A, Lang M, Kuusk J. Database of optical and structural data for the validation of forest radiative transfer models. In: Kokhanovsky AA, Ed. Radiative transfer and optical properties of atmosphere and underlying surface. Light scattering reviews 7. Springer: Berlin 2013; pp. 109-48.

[24] Kuusk A, Lang M, Kuusk J, *et al*. Database of optical and structural data for the validation of radiative transfer models. Technical report Ver. 09.2014. Tartu Observatory, 2014. Available from: http://www.aai.ee/bgf/jarvselja_db/jarvselja_db.pdf

[25] Niinemets U, Kull K. Leaf weight per area and leaf size of 85 Estonian woody species in relation to shade tolerance and light availability. Forest Ecol Manag 1994; 70: 1-10.

[26] Repola J. Biomass equations for birch in Finland. Silva Fennica 2008; 42(4): 605-24.

[27] Repola J. Biomass equations for Scots pine and Norway spruce in Finland. Silva Fennica 2009; 43(4): 625-47.

[28] Demarez V, Duthoit S, Baret F, Weiss M, Dedieu G. Estimation of leaf area and clumping indexes of crops with hemispherical photographs. Agric For Meteorol 2008; 148(4): 644-55.

[29] Kuusk A, Kuusk J, Lang M, Lükk T. Vicarious calibration of the PROBA/CHRIS imaging spectrometer. The Photogramm J Finland 2010; 22(1): 46-59.

[30] Vermote EF, Tanre D, Deuze JL, Herman M, Morcrette JJ. Second simulation of the satellite signal in the solar spectrum, 6S: An overview. IEEE Trans Geosci Remote Sens 1997; 35(3): 675-86.

[31] Thenkabail PS, Enclona EA, Ashton MS, Legg C, De Dieu MJ. Hyperion, IKONOS, ALI, and ETM+ sensors in the study of African rainforests. Remote Sens Environ 2004; 90(1): 23-43.

[32] Huang J, Zeng Y, Kuusk A, *et al*. Inverting a forest canopy reflectance model to retrieve the overstorey and understorey leaf area index for forest stands. Int J Remote Sens 2011; 32(22): 7591-611.

[33] Knyazikhin Y, Glassy J, Privette JL, *et al*. MODIS leaf area index (LAI) and fraction of photosynthetically active radiation absorbed by vegetation (FPAR) product (MOD15) algorithm theoretical basis document; 1999. Available from: http://eospso.gsfc.nasa.gov/atbd/modistables.html

[34] GRASS. GRASS Development Team, GRASS 7.0.svn Reference Manual; 2012. Available from: http://grass.osgeo.org/grass70/manuals/html70_user/

[35] Kuusk A. A Markov chain model of canopy reflectance. Agric For Meteorol 1995; 76(3-4): 221-36.

[36] Kuusk A. The hot spot effect in plant canopy reflectance. In: Myneni RB, Ross J, Eds. Photon-vegetation interactions. applications in optical remote sensing and plant ecology. Springer: Berlin 1991; pp. 139-59.

[37] Ross J. The radiation regime and architecture of plant stands. Dr. W. Junk Publishers: The Hague 1981.

[38] Nilson T. A theoretical analysis of the frequency of gaps in plant stands. Agr Meteorol 1971; 8: 25-38.

[39] Kuusk A, Kuusk J, Lang M. Modeling directional forest reflectance with the hybrid type forest reflectance model FRT. Remote Sens Environ 2014; 149: 196-204.

[40] Nilson T, Kuusk A. Improved algorithm for estimating canopy indices from gap fraction data in forest canopies. Agric For Meteorol 2004; 124(3-4): 157-69.

[41] Press WH, Teukolsky SA, Vetterling WT, Flannery BP. Numerical recipes in FORTRAN. The art of scientific computing. UK: Cambridge University Press 1992.

Received: December 06, 2014 Revised: January 21, 2015 Accepted: February 02, 2015